Adaptive gene loss in the common bean pan-genome during range expansion and domestication

Cortinovis, G.[1*], Vincenzi, L.[2*], Anderson, R.[3], Marturano, G.[2], Marsh, J.I.[3], Bayer, P.E.[3], Rocchetti, L.[1], Frascarelli, G.[1], Lanzavecchia, G.[1], Pieri, A.[1], Benazzo, A.[4], Bellucci, E.[1], Di Vittori, V.[1], Nanni, L.[1], Ferreira Fernández, J.J.[5], Rossato, M.[2, 6], Aguilar, O.M.[7], Morrell, P.L.[8], Rodriguez, M.[9], Gioia, T.[10], Neumann, K.[11], Alvarez Diaz, J.C.[12], Gratias-Weill, A.[12], Klopp, C.[13.], , Geffroy, V.[12], Bitocchi, E.[1], Delledonne, M. [2, 6*], Edwards, D.[3*], Papa, R [1*#].

[1] Department of Agricultural, Food and Environmental Sciences, Marche Polytechnic University, 60131 Ancona, Italy

[2] Department of Biotechnology, University of Verona, 37134 Verona, Italy

[3] Centre for Applied Bioinformatics and School of Biological Sciences, University of Western Australia, Perth, WA 6009, Australia

[4] Department of Life Sciences and Biotechnology, University of Ferrara, 44100 Ferrara, Italy

[5] Regional Service for Agrofood Research and Development (SERIDA), Ctra AS-267 PK 19, 33300 Asturias, Spain

[6] Genartis s.r.l., 37126 Verona, Italy

[7] Institute of Biotechnology and Molecular Biology, UNLP-CONICET, CCT La Plata, La Plata, Argentina

[8] Department of Agronomy and Plant Genetics, University of Minnesota, 55108-6026, St. Paul Minnesota, USA

[9] Department of Agriculture, University of Sassari, 07100 Sassare, Italy

[10] School of Agricultural, Forestry, Food and Environmental Sciences, University of Basilicata, 85100 Potenza, Italy

[11] Leibniz Institute of Plant Genetics and Crop Plant Research (IPK), 06466 Seeland, Germany

[12] CNRS, INRAE, Institute of Plant Sciences Paris-Saclay (IPS2), Univ Evry, University Paris-Saclay, Orsay 91405, France

[13] INRAE, Genotoul Bioinformatics Platform, Applied Mathematics and Informatics of Toulouse, Sigenae, MIAT UR875, Castanet Tolosan, France

[*] These authors contributed equally to this work

[#] Corresponding authors

Abstract

The common bean (*Phaseolus vulgaris* L.) is an important grain legume crop [1,2] whose life history offers an ideal evolutionary model to identify adaptive variants suitable for breeding programs [3]. Here we present the first common bean pan-genome based on five high-quality genomes and whole-genome reads representing 339 genotypes. We found ~243 Mb of additional sequences containing 7,495 protein-coding genes missing from the reference, constituting 51% of the total presence/absence variations (PAVs). There were more putatively deleterious mutations in PAVs than core genes, probably reflecting the lower

effective population size of PAVs as well as fitness advantages due to the purging effect of gene loss. Our results suggest pan-genome shrinkage occurred during wild range expansion from Mexico to South America, with more PAV loss per individual in Andean vs Mesoamerican populations. Selection during wild spreading and domestication was also associated with PAV loss involved in important adaptive traits. Our findings provide evidence that partial or complete gene loss was a key adaptive trait leading to localized and genome-wide reductions. This departs from established paradigms and reveals how evolutionary forces shape gene composition within plant genomes. The common bean pan-genome offers a valuable resource for legume research and breeding, climate change mitigation, and sustainable agriculture.

Main

Food legumes provide valuable genetic resources to address agriculture-related societal challenges, including climate change mitigation, biodiversity conservation, and the need for sustainable agriculture and healthy diets [4-7]. The common bean (*Phaseolus vulgaris* L.) is a diploid (2n=2x=22) and predominantly self-pollinating annual grain legume crop with a prominent role in agriculture and broader societal importance [1,2]. It is also a useful model of crop evolution [3] reflecting the parallel and independent life history of two geographically isolated and genetically differentiated gene pools (Mesoamerican and Andean) following the expansion of wild from Mexico to South America ~150,000–200,000 years ago, an order of magnitude earlier than its dual domestication [8-11]. Previous studies using a single reference genome have provided insights into the population structure of the common bean [12] and the genetic basis of important adaptive traits [13]. However, pan-genomic diversity must be explored to gain a comprehensive understanding [14-17]. We therefore constructed the first *P. vulgaris* pan-genome using a non-iterative approach and investigated its genetic variation in terms of PAVs within a representative panel of genetically and phenotypically well-characterized accessions. This publicly available common bean pan-genome provides a valuable starting point to identify genes and genomic mechanisms affecting adaptation and will accelerate legume improvement.

Characterization of the common bean pan-genome

To generate the common bean pan-genome, we applied a non-iterative approach to five high-quality *de novo* genome assemblies of wild and domesticated genotypes and incorporated short-read whole genome sequencing (WGS) data from 339 representative common bean accessions, comprising 33 wild and 306 domesticated forms. This revealed ~242 Mb of additional sequence containing 7,495 genes missing from the reference genome. The new sequences account for 22% of all discovered genes, with 9% (3,040 genes) derived from the high-quality genomes and the remaining 13% (4,455 genes) from the panel of 339 WGS genotypes. The final size of the reconstructed pan-genome was ~780 Mb, with 34,928 predicted protein-coding genes (**Supplementary Table 1a**).

69 The new reference pan-genome was used for both variant calling and PAV calling (**Supplementary**
70 **Table 1b**). We detected 23,343,365 variant sites, 19,002,047 of which were classified as single-nucleotide
71 variants (SNVs) and 4,341,318 as insertions/deletions (InDels). Following PAV calling, the categorization of
72 all 34,928 predicted genes by frequency unveiled that 58% of the pan-genome consists of core genes found
73 across all lines (20,369 genes), with the remaining 42% comprising PAVs. These PAVs are either partially
74 shared among accessions or exclusive to a single genotype, totalling 14,559 genes (**Supplementary Table**
75 **1c**). Notably, 51% of these PAVs originate from non-reference regions (NRRs), representing sequences
76 absent in the reference genome. The growth curve related to the size calculation suggested a closed pan-
77 genome. In agreement, the pan-genes reached the saturation point (99%, 34,579 genes) and remained
78 constant without substantial increase when the number of accession genomes exceeded 120. In contrast,
79 the size of the core genes decreased with each added genotype (**Fig. 1a**). This indicates that the final pan-
80 genome includes almost all the gene content of *P. vulgaris*. Gene Ontology (GO) enrichment analysis
81 showed that the core genes are significantly enriched for terms associated with homeostatic (GO:0042592)
82 and catabolic (GO:0043632) processes (**Supplementary Fig. 1a; Supplementary Table 1d**) whereas the
83 PAVs are significantly enriched for terms related to defence (GO:0006952), responses to external stimuli
84 (GO:0009605), responses to light (GO:0019684), and reproduction (GO:0000003, GO:0022414)
85 (**Supplementary Fig. 1b; Supplementary Table 1e**).
86 To investigate the evolution of the core genes and PAVs, we calculated the non-synonymous and
87 synonymous ratio (Ka/Ks) for each gene in each accession (**Supplementary Table 1f**). This revealed a
88 statistically significant difference ($p < 2.2 \times 10^{-16}$), with the PAVs including a greater number of harmful
89 variants relative to benign variants when compared to the core genes (**Supplementary Fig. 1c;**
90 **Supplementary Table 1g**). When we split the PAVs into three subcategories based on their frequency (*soft-*
91 *core* 0.90 ≤ freq. < 1; *accessory* 0.10 ≤ freq. < 0.90; and *rare* freq. < 0.10), we observed a significant increase
92 ($p = 0.048$) in the proportion of putative harmful variants among the rare genes compared to the soft-core
93 genes (**Fig. 1b; Supplementary Table 1g**). These results may reflect the lower effective population size of
94 the PAVs (reducing the efficiency of purifying selection) and/or the higher fitness gain from purging genes
95 that have accumulated deleterious mutations (loss-of-function mutations).
96
97 **Evolutionary trajectory of the common bean**
98 The common bean is characterized by three eco-geographic gene pools. The two major ones are the
99 Mesoamerican (M) and Andean (A) populations, which encompass both wild and domesticated forms. The
100 third originates from Northern Peru/Ecuador (PhI) and has a relatively narrow distribution of only wild
101 individuals [11]. The Mesoamerican and Andean gene pools include five domesticated subgroups (M1, M2,
102 A1, A2 and A3) corresponding to the Jalisco-Durango, Mesoamerica, Nueva Granada, Peru, and Chile races
103 [13]. We constructed a neighbour-joining (NJ) phylogenetic tree (**Fig. 2a**) and conducted PAV-based

104 principal component analysis (PCA) (**Fig. 2b**), both of which confirmed this well-defined population
105 structure. Both analyses further divided the M1/Jalisco-Durango races into two clusters that we named
106 cluster A and cluster B, respectively. The analysis of variance conducted on M1/Jalisco-Durango accessions,
107 considering the first component for the days to flowering, revealed that cluster A is significantly later-
108 flowering than cluster B (**Fig. 2c; Supplementary Table 2a**). The Jalisco (cluster A) and Durango (cluster B)
109 races are therefore genetically distinguishable based on photoperiod sensitivity. This outcome also
110 confirmed that our pan-genome enhances the characterization of genetic diversity and improves its
111 analysis, exploitation and management. Cumulatively, the first and the second principal components of the
112 PAV-based PCA explained 47.2% of the total variance, where PC1 mainly defined the differences between
113 Mesoamerican and Andean gene pools while PC2 split the groups and subgroups within each gene pool
114 (**Fig. 2b**). The NJ tree further underscored the suitability of core genes for phylogenetic reconstruction
115 because they mitigate biases arising from the absence of genetic material among the compared accessions.
116 In contrast to the tree based on single-nucleotide polymorphisms (SNPs) located on PAVs (**Supplementary**
117 **Fig. 2a**), the NJ tree based solely on core SNPs properly grouped the wild PhI accession close to the wild
118 Mesoamerican genotypes originating from Guatemala and Costa Rica (**Fig. 2a**), which are most closely
119 related to the PhI gene pool [11].

120 When we examined the total number of PAVs per genetic group (**Supplementary Table 2b**), we
121 found that the wild Mesoamerican and Andean populations have more PAVs compared to their
122 domesticated counterparts (**Fig. 2d**). This supports the well-established notion that domestication is usually
123 associated with a reduction of genetic diversity. The amplification of gene loss in domesticated common
124 bean could reflect a classic bottleneck effect rather than natural selection [18]. We also found that the
125 M1/Jalisco-Durango and A2/Peru races have more PAVs than the other subgroups in the same gene pool
126 (**Fig. 2d**). This was supported by nucleotide diversity analysis applied to the 1,451,663 core SNPs (**Fig. 2e**;
127 **Supplementary Table 2c**) and agrees with a recent hypothesis proposing that the M1/Durango-Jalisco and
128 A2/Peru races were the first domesticated Mesoamerican and Andean populations from which the M2, A1
129 and A3 races arose during a secondary domestication phase [13].

130 To study inter-gene-pool hybridization, the PAV matrix for American domesticated accessions was
131 analysed by using Fisher's exact test to compare the Mesoamerican and Andean populations. We found
132 5,556 PAVs (65% of the total) with a statistically significant difference in frequency ($p < 0.05$) between the
133 two gene pools. These included 778 diagnostic PAVs, 91% (707) of which were fixed in the Mesoamerican
134 gene pool and 9% (71) in the Andean gene pool (**Supplementary Table 2d**). GO enrichment analysis applied
135 to the 778 diagnostic genes revealed enrichment in processes related to detoxification (GO:0098754),
136 metabolism (GO:0008152), and responses to stimuli (GO:0050896) (**Supplementary Fig. 2b**). Interestingly,
137 none of these PAVs were found to be diagnostic between gene pools in Europe (**Supplementary Table 2d**),
138 and when Fisher's exact test was applied to the subset of 114 European accessions, we did not detect any

139 diagnostic genes between the Mesoamerican and Andean gene pools (**Supplementary Table 2e**). These
140 outcomes clearly reflect the extensive inter-gene-pool hybridization in European germplasm and confirm its
141 key role in the adaptation of common bean to new agricultural environments [13].

142 To investigate the influence of PAVs on important trait variations and identify candidate genes
143 associated with them, we conducted a PAV-based genome-wide association study (GWAS) involving 218
144 American and European domesticated genotypes. We identified 39 significative association events
145 correlated with day-to-flowering and photoperiod sensitivity, previously detailed in [13]. These associations
146 were linked to 35 potential candidate PAVs, highlighting their likely involvement in regulating floral
147 transition (**Supplementary Table 2f**). An interesting example is the GWAS peak associated with flowering
148 time and photoperiod sensitivity located on Phvul.003G185200 (Chr03:40,838,810-40,850,729). This PAV
149 demonstrates orthology to the *HDA5* gene in *Arabidopsis thaliana*, which displays deacetylase activity.
150 Notably, *A. thaliana* mutants with impaired HDA5 expression patterns manifest late-flowering phenotypes
151 due to the up-regulation of two floral repressor genes, namely FLOWERING LOCUS C (FLC) and MADS
152 AFFECTING FLOWERING 1 (MAF1) [19]. It is noteworthy that common bean genotypes lacking the PAV
153 Phvul.003G185200 exhibit early flowering phenotypes compared to those accessions carrying the gene
154 (**Supplementary Fig. 2c**), implying an adaptive role correlated to the loss. Furthermore, we found that 9 out
155 of the 35 candidate PAVs for GWA analysis show signature of selection in various comparisons, specifically,
156 two PAVs between wild and domesticated Mesoamerican populations and seven PAVs between wild and
157 domesticated Andean populations. Overall, although the majority (59%) of the candidate PAVs were
158 located on the reference genome, a significant 41% were situated on the NRRs (**Supplementary Table 2f**),
159 reaffirming the efficacy of the pan-genome in identifying functional variants associated with economically
160 or evolutionarily important traits.

161

162 **Pan-genome shrinkage during wild expansion to South America**

163 One of the most striking outcomes we observed was the difference in pan-genome size between the
164 Mesoamerican and Andean gene pools (**Fig. 3a**). We calculated the total number of PAVs per individual and
165 found that accessions from the same gene pool clustered together in separate groups, with Mesoamerican
166 accessions featuring more PAVs per accession than Andean ones (**Fig. 3b, c; Supplementary Table 3a**). One
167 possible explanation is that this reduction in pan-genome size may simply reflect genetic drift and the two
168 sequential bottlenecks that occurred solely in the Andean population [12]. To better understand the roles
169 of different evolutionary forces in shaping the PAV content of the Mesoamerican and Andean gene pools,
170 and to distinguish between the effects of adaptation, population demography and history, we first focused
171 on the analysis of wild accessions. Considering a panel of wild genotypes representing the entire
172 geographical distribution in Latin America, we applied bivariate fit analysis and found a significant
173 correlation ($p < 0.0001$) between the number of PAVs per individual and the latitude. Analysis of variance in

174 which wild individuals were grouped by latitude followed by spatial interpolation revealed a significant and
175 progressive loss of genes ranging from the accessions of Northern Mexico to those of Northwestern
176 Argentina (**Fig. 4a, b; Supplementary Table 3b**). Furthermore, F_{ST} analysis on PAVs comparing
177 Mesoamerican and Andean wild populations may suggests the occurrence of selection for gene loss during
178 wild range expansion (**Fig. 4c**). We found that 64% of all candidate PAVs in the top 5% of the F_{ST} distribution
179 (Fst≥0.85) are absent in the wild Andean gene pool. This high rate of gene loss in the Andean population
180 significantly exceeds the gene loss rate observed in the entire variable genome (26%), demonstrating a
181 more than twofold increase. This difference in gene loss rates was statistically validated using bootstrap
182 resampling, strongly suggesting that gene loss during the process of wild differentiation was not a random
183 occurrence but evident outcome of selective forces (**Supplementary Fig. 3a, b**). Moreover, functional
184 annotation of the candidate PAVs revealed the enrichment of genes involved in pollen germination, innate
185 immunity, abiotic stress tolerance, and root hair growth, indicating a potential adaptive role
186 (**Supplementary Table 3c**). Overall, our findings suggest that selective pressure favouring the loss of genes
187 involved in adaptive mechanisms, coupled with the influence of genetic drift resulting from the founder
188 effect, may have contributed to the shrinking of the Andean pan-genome during wild differentiation.
189
190 **Footprints of selection for gene loss during domestication**
191 The PAVs putatively shaped by selection during domestication in Mesoamerica and the Andes revealed
192 further evidence that gene loss underpinned the successful adaptation of the American common bean. F_{ST}
193 analysis was applied to PAVs in wild and domesticated forms (separately for each gene pool) with only PAVs
194 in the top 5% of the F_{ST} distribution considered as candidates. We found 460 PAVs potentially under
195 selection in the Mesoamerican population ($F_{ST} \geq 0.31$) and 514 in the Andean population ($F_{ST} \geq 0.27$)
196 (**Supplementary Table 4a, b**). Functional annotation of the candidate PAVs revealed the enrichment of
197 genes associated with domestication syndrome and adaptive traits such as dormancy, floral transition, light
198 acclimation, defence, and symbiotic interactions (**Supplementary Table 4c, d**). Importantly, the candidate
199 Phvul.003G265200 (Chr03: 50,365,995-50,368,501) is orthologous to 11 members of the plant Rho GTPase
200 subfamily (ROP), including *ROP6* encoding a small Rho-like GTP binding protein. This GTPase subfamily is
201 required for symbiotic interactions [20-22], and in the plasma membrane of *Lotus japonicus* cells it interacts
202 directly with NOD FACTOR RECEPTOR 5, one of two nodulation factor receptors essential for nodule
203 formation during symbiosis [23]. From our analysis, Phvul.003G265200 is a putative selected PAV (F_{ST} =
204 0.50) for the Mesoamerican gene pool whose frequency declined by more than 60% during progression
205 from the wild (0.94) to the domesticated (0.25) population (**Supplementary Table 4a**). Overall, no
206 significant differences were observed in terms of absences between the wild and domesticated populations
207 of both gene pools. However, a significant proportion of PAVs putatively under selection, specifically 63%
208 (289 genes) in the Mesoamerican population (**Fig. 5a**) and 80% (411 genes) in the Andean one (**Fig. 5b**),

were less frequent in domesticated than wild populations. When considering all PAVs, the percentage of PAVs with lower frequencies in domesticated populations fell significantly to 22% ($p < 2.2 \times 10^{-16}$) for the Mesoamerican gene pool and 29% ($p < 2.2 \times 10^{-16}$) for the Andean one (**Fig. 5a, b**). These findings suggest that selection during domestication resulted in gene loss, but unlike the range expansion of wild populations, it did not completely abolish the selected genes. This may reflect the different evolutionary timescales involved: wild differentiation occurred ~150,000 years ago whereas domestication was much more recent at ~8,000 years ago. These findings are consistent with previous observations that selection during the domestication of common bean in Mesoamerica has directly affected the transcriptome, leading to a ~20% decrease in gene expression levels attributed to loss-of-function mutations [18]. We also detected 29 PAVs with high F_{ST} values in common between the Mesoamerican and the Andean gene pools, and these are mainly associated with the tryptophan metabolic pathway. Tryptophan holds significance as a precursor in secondary metabolism, contributing to the synthesis of essential molecules like auxin, serotonin, and melatonin. These compounds play diverse roles in plant physiology, influencing processes such as seed germination, root development, senescence, and flowering. Additionally, they contribute to the plant's response mechanisms against both biotic and abiotic stresses [24]. We analysed their frequencies and found that ~86% in both gene pools decreased in frequency during the progression from wild to domesticated accessions (**Supplementary Table 4e**). This may indicate a pattern of genomic convergence for some key adaptive genes between the Mesoamerican and Andean populations during their parallel domestication events.

Conclusions

The global economic and social importance of the common bean means that pan-genomic analysis could boost the conservation and exploitation of its genetic resources to address key challenges in agriculture and wider society [1-6]. The genotypes selected for this study encompass both wild and domesticated forms, ensuring that the pan-genome comprehensively captures the extensive genetic variation within this species. This publicly accessible tool serves as a valuable resource for studies in population genetics, functional genomics, and plant breeding. PAV analysis provided insight into the evolutionary dynamics of pan-genome adaptation, including putative signals of selection for complete gene loss during wild differentiation between the Mesoamerican and Andean gene pools, contributing to the smaller pan-genome of the Andean population. We also identified putative selection footprints for partial gene loss during both domestication processes in Mesoamerica and the Andes, causing localized reductions in gene frequencies in domesticated populations compared to their wild counterparts. Candidate genes that have been completely or partially lost appear to be involved in important adaptive mechanisms, such as flowering time, symbiosis, biotic and abiotic stress tolerance, and root hair growth.

243 The significant role of reductive genome evolution in adaptation is now widely recognized [25-27]. For
244 instance, in contrast to their European native counterparts, invasive genotypes exhibited a reduced
245 genome size resulting in phenotypic effects that enhanced the species' invasive potential. This included an
246 accelerated early growth rate driven by a negative correlation between genome size and the rate of stem
247 elongation [28]. Similarly, Díez et al. [29] documented the genome size variations within the *Zea mays*
248 species during the post-domestication process, revealing that maize landraces have significantly smaller
249 genome sizes compared to their closest wild relatives, the teosintes. Notably, a negative correlation
250 between maize genome size and altitude was observed [29]. Moreover, gene loss is considered functionally
251 equivalent to other loss-of-function mutations, such as premature stop codons, providing an important
252 source of adaptive phenotypic diversity [30-33]. A notable example is found in *A. thaliana*, where loss of
253 function mutations in the *SCARECROW* (*SCR*) and/or SnRK2-type protein kinase (*SRK*) genes underlie the
254 switch from obligate outcrossing (self-incompatibility) to self-fertilization [34]. This transition is widely
255 recognized as one of the predominant evolutionary shifts among flowering plants, allowing the successful
256 colonization of oceanic islands, an ecological principle known as Baker's rule. Accordingly, under the
257 influence of specific and diverse agro-ecological pressures, the relinquishment of particular genes can
258 confer a selective advantage on a given population. Overall, our findings support the "less is more"
259 hypothesis in which non-functionalization is a common adaptive response [35]. This may be relevant when
260 populations face selective pressure resulting from radical environmental changes, such as the expansion of
261 wild common bean from the warm and humid climate of Central Mexico to higher and cooler altitudes in
262 the Andes. Our results therefore establish a novel scenario in which evolutionary forces drive partial or
263 complete gene loss due to selective pressure favouring adaptation rather than responses to stochastic
264 events only. Mutations are more likely to cause a loss rather than a gain of function, so adaptive gene loss
265 provides a rapid evolutionary response to environmental changes. This has profound implications for
266 strategies to mitigate climate change. The common bean pan-genome is a valuable starting point that will
267 lead to a deeper understanding of the genetic variations and genome dynamics responsible for key
268 adaptive traits in food legumes.
269

270 ## Methods

271 ### Sources of genetic diversity

272 The pan-genome was constructed from five high-quality genomes representing the Mesoamerican and
273 Andean gene pools. The *P. vulgaris* reference genome Pvulgaris_442_v2.0 (PV442) was downloaded from
274 Phytozome (https://phytozome-next.jgi.doe.gov/), the genomes of BAT93 and JaloEPP558 were provided
275 by the INRAE Institute, and the genomes of MIDAS and G12873 were sequenced and assembled *de novo*
276 specifically for this study (**Supplementary Table 5a**). We also integrated 339 representative low-coverage
277 WGS common bean genotypes, including 220 domesticated and 10 wild accessions from previous studies

278 [11, 13]. The remaining 109 accessions were multiplied in the greenhouse, and DNA extracted from young
279 leaves was used for sequencing (**Supplementary Table 5b**).
280
281 **Plant growth and DNA extraction**
282 MIDAS and G12873 single seed descent (SSD) genotypes were multiplied in the greenhouse. For both
283 samples, 2 g of young leaf material was collected after 48 h of dark treatment and high-molecular-weight
284 (HMW) DNA was extracted as previously described [36]. DNA quality was evaluated according to Oxford
285 Nanopore Technologies (ONT) requirements. Specifically, purity was assessed using a NanoDrop 1000
286 spectrophotometer (Thermo Fisher Scientific), the concentration was determined using a dsDNA Broad
287 Range Assay Kit with Qubit 4.0 (Thermo Fisher Scientific), and the fragment size (≤ 400 kb) was determined
288 using the CHEF Mapper electrophoresis system (Bio-Rad Laboratories). Fragments < 25 kb were removed
289 using the Short Reads Eliminator kit (Circulomics) leaving 75% of the DNA from the MIDAS samples and 95%
290 from the G12873 samples.
291 *P. vulgaris* genotypes of BAT93 and JaloEEP558 were sowed in soil and grown in a growth chamber at 23°C,
292 75% humidity, and 8 h dark and 16 h light photoperiods under fluorescent tubes (166lE). Young trifoliate
293 leaves of BAT93 and JaloEEP558 genotypes were collected and flash-frozen with liquid nitrogen. Three days
294 before sampling, plants were dark treated to optimize the high molecular weight DNA extraction. In
295 addition, 109 SSD accessions were multiplied in the greenhouse and young leaves were collected in silica
296 gel for drying and subsequent DNA extraction using the DNeasy 96 Plant kit (Qiagen) according to the
297 manufacturer's instructions. For each sample, 50–70 mg of dried leaf material was pulverized with a Tissue-
298 Lyser II (Qiagen) at 30 Hz for 6 min. The DNA quality and quantity were evaluated using a NanoPhotometer
299 NP80 (Implen), and the concentration was determined using a Qubit BR dsDNA assay kit (Thermo Fisher
300 Scientific).
301
302 **Sequencing low-coverage WGS accessions**
303 DNA libraries for all samples were prepared using a KAPA Hyper Prep kit and PCR-free protocol (Roche). For
304 each genotype, 200 ng of DNA was fragmented by sonication using a Covaris S220 device (Covaris) and
305 WGS DNA libraries were generated using a 0.7–0.8× ratio of AMPureXP beads for final size selection.
306 Libraries were quantified using the Qubit BR dsDNA assay kit and equimolar pools were quantified by real-
307 time PCR against a standard curve using the KAPA Library Quantification Kit (Kapa Biosystems). Libraries
308 were sequenced on the NovaSeq 6000 Illumina platform in 150PE mode, producing 15–30 million
309 fragments per sample.
310
311 **Sequencing and assembly of MIDAS and G12873 genomes**

312 Following quality control and priming according to ONT specifications, libraries were sequenced on a
313 MinION device with a SpotON flow cell (FLO-MIN106 R9.4.1-Rev D). Two libraries were prepared for each
314 genotype according to the SQK-LSK109 ligation sequencing protocol (ONT) with minor adjustments. Each
315 library was loaded twice, and the flow cell was washed using the Flow Cell Wash Kit (ONT). Illumina PCR-
316 free libraries were prepared starting with 1 ug of fragmented gDNA using the KAPA Hyper prep protocol.
317 This process involved extending the adapter ligation time up to 30 minutes and conducting post-clean-up
318 size selection using 0.7X AMPure XP beads. The library's concentration and size distribution were assessed
319 using a Bioanalyzer 2100 in combination with high-sensitivity DNA reagents and chips. Sequencing was
320 performed on a NovaSeq6000 instrument to generate 150-bp paired-end reads. MIDAS and G12873 whole-
321 genome assemblies were generated using the nanopore-based approach based on 26 Gb (50-fold coverage)
322 and 36 Gb (69-fold coverage), respectively. Raw nanopore reads were corrected using Canu v2.1 [37] and
323 the resulting corrected reads were assembled *de novo* using wtdbg2 v2.5 [38]. Draft assemblies were
324 refined by iterative polishing using long reads (Racon v1.4.3 and Medaka v1.0.3) [39] and short reads (three
325 rounds of Pilon v1.23) [40]. Completeness was assessed using BUSCO v4.1.2 [41] and the Fabales_odb10
326 dataset (**Supplementary Table 5c**).
327
328 **Sequencing and assembly of BAT93 and JaloEEP558 genomes**
329 High molecular weight DNA of BAT93 and JaloEEP558 genotypes was sequenced with a PacBio Sequel II
330 system by GENTYANE platform (INRAE Clermont-Ferrand, France). A total of 21.09 and 29.35 Gb of PacBio
331 HiFi reads were generated from BAT93 and JaloEEPP558, respectively. PacBio HiFi reads were *de novo*
332 assembled into contigs using HiFiasm (v 0.9.0) with default parameters [42].
333
334 **Orthologous/paralogous analysis and clustering threshold settings**
335 To incorporate two distinct populations, namely the Andean and the Mesoamerican gene pools, into the
336 pangenome, precise differentiation between orthologous and paralogous genes is imperative.
337 Consequently, a meticulous strategy was devised to ensure the preservation of solitary orthologous gene
338 copies along with all paralogous counterparts. The relationship between orthologous genes was calculated
339 with minimap2 v2.17 [43] to align the MIDAS and G12873 genome assemblies using the open reading
340 frames (ORFs) of 2,330 complete single-copy BUSCO (Benchmarking Universal Single-Copy Orthologs) genes
341 selected from the *P. vulgaris* reference genome PV442 (**Supplementary Table 5d**). The percentage identity
342 was calculated for each ORF based on the number of matches in the alignments as a proportion of ORF
343 length. The relationship between paralogous genes was calculated using the three most abundant gene
344 families (OG0000273, OG0000328, and OG0000085) in the *P. vulgaris* PV442 reference genome, composed
345 of 26, 37, and 42 genes, respectively. An all-versus-all comparison between the members of the same
346 family was implemented using minimap2. The percentage of identity was calculated for each gene family

347 by dividing the number of matches in the alignments by the reference gene ORF length and then averaging
348 the identity percentages for each family. Finally, the results of both tests were used to establish a clustering
349 threshold of 90% to retain only one orthologous and all paralogous genes in the pan-genome
350 (**Supplementary Table 5e**).
351
352 **Pan-genome construction**
353 We used a paired genome alignment strategy for pan-genome construction [44]. The PV442 reference
354 genome was independently mapped onto MIDAS, G12873, BAT93 and JaloEPP558 with minimap2 v2.17
355 using the alignment pre-set *-x asm5*, which considers regions with an average divergence < 5%. The bam
356 files of the four alignments were converted to delta files and structural variants were called using
357 Assemblytics v 1.2.1 [45]. Only deletions were selected as NRRs [44]. Uncovered contigs private to the four
358 analysed genomes were identified by applying samtools depth v1.1 [46] to the bam files and were
359 extracted as NRRs. Deletions and uncovered contigs were independently filtered for a minimum length of 1
360 kb and clustered using CD-HIT-EST v4.8.1 [47] with a sequence identity of 90%, as described above for the
361 orthologous and paralogous genes. To ensure that the NRRs identified through this method didn't
362 encompass orthologous genes already existing in the PV442 reference genome, we specifically employed
363 highly conserved BUSCO genes. We conducted a comparative analysis between the full complement of
364 4,947 MIDAS and 4,812 G12873 BUSCO genes present in PV442 and the NRRs derived from MIDAS and
365 G12873 using BLASTp. Illumina data representing the 339 low-coverage WGS common bean accessions
366 were trimmed with fastp v0.21.0 [48] and aligned to the preliminary pan-genome using bowtie2 v2.3.5.1
367 [49] with default parameters. The unmapped reads from these alignments were extracted using samtools
368 v1.11, assembled using MaSuRCA v3.4.2 [50] with default parameters, and clustered using CD-HIT-EST
369 v4.8.1 with a sequence identity of 90%. Finally, the NRRs derived from the panel of 339 common bean
370 accessions were added to the preliminary pan-genome to generate the final pan-genome. To exclude
371 putative contaminants and/or organelle sequences, NRRs were compared to the NCBI non-redundant
372 nucleotide database using BLASTn, considering a minimum 80% identity and 25% coverage, leading to the
373 removal of 1,194 sequences. Overall, we identified 64,174 added sequences, 86% of which reflected the
374 mapping of the 339 low-coverage WGS accessions. The remaining 14% was identified by comparing the
375 reference genome independently with the other four high-quality genomes (**Supplementary Table 1a**).
376
377 **Pan-genome annotation**
378 Repetitive sequences were identified and soft-masked using RepeatModeler v2.0.2 [51] and RepeatMasker
379 v4.1.2-p1 [52]. Protein-coding genes were identified using a hybrid-approach prediction with Augustus
380 v3.3.3 [53]. Proteins from *P. vulgaris* and correlated species (*Medicago truncatula* and *Glycine soja*) plus
381 RNA-Seq data (unpublished data from [18]) were aligned to the genome and used as extrinsic evidence.

382 Protein sequences were aligned with Hisat2 v2.2.1 [54] and RNA-Seq data were aligned using Genome
383 Threader v1.7.1 [55]. BUSCO genes in the Fabales_odb10 database were used to train the model for the
384 Augustus predictor. Predicted genes were scanned with InterProScan v5.46-81.0 [56] for the presence of
385 protein domains. Using a custom script, genes with transposon-related domains were filtered out and
386 retained in the annotation if they contained at least one known protein domain. The filtered proteins were
387 compared to the pan-genome with BLASTp v2.12.0 [57] and filtered by the best hits. The predicted genes
388 were clustered with the proteins of all species considered in the annotation using OrthoFinder v2.5.4 [58].
389 Finally, functional annotation was achieved by integrating information about orthologous genes and by
390 identifying functional domains using a custom script.
391
392 **PAV calling**
393 Illumina data representing the 339 low-coverage WGS accessions were aligned to the pan-genome using
394 bowtie2 v2.3.5.1 and the coverage of each predicted gene was calculated for each accession using samtools
395 v1.11 (**Supplementary Table 5f**). PAV calling thresholds were defined for each accession according to the
396 minimum coverage value of 1000 randomly selected BUSCO genes (ORFs). The BUSCO genes are
397 orthologous genes that should be present in all considered accessions, but a few underrepresented genes
398 in a given accession could constitute a bias. To avoid this, values below 1% (the 10 least covered genes)
399 were discarded. The identified genes were classified based on their frequency as core genes if present in all
400 the accessions or PAVs if partially shared or private to a single genotype (**Supplementary Table 1b, c**).
401
402 **Pan-genes and core genes size calculation**
403 The curves describing the pan-genome and core genome sizes were evaluated by considering 1,000 random
404 orders of the 339 genotypes. The orders were chosen randomly among all possible permutations (n! where
405 n=[1,339]). For each ordering, the gene sets of the accessions were progressively added to the total
406 genome size without considering the genes already present in the total set. The same procedure was
407 applied for the core genome size, but the gene sets were intersected when each genome was added, thus
408 keeping only the genes in common for each iteration (**Supplementary Table 5g, h**).
409
410 **Variant calling**
411 SNVs and InDels were called with bcftools v1.10.2 [59] based on the alignment of 339 accessions with the
412 pan-genome using bowtie2 v2.3.5.1. We used bcftools mpileup v1.10.2 to generate a genotype likelihood
413 table, and variants were identified using bcftools call v1.10.2 and the pileup table, producing the final vcf
414 file.
415
416 **Non-synonymous and synonymous mutations**

417 The Ka/Ks ratio was computed for each gene in each accession using KaKs calculator v2.0 [60]. For each
418 gene, the consensus sequence of each accession was extracted using bcftools consensus v1.10.2. The
419 calculator compares the pan-genome gene sequence with the gene sequence of each accession to identify
420 non-synonymous and synonymous variants and then computes the ratio. The calculator reported *NA* when
421 there were no variants in a specific accession or when the denominator of the Ka/Ks ratio was zero. It was
422 possible to compute the analysis for 30,850 of 34,928 genes. Sometimes the length of one of the two
423 compared sequences was not divisible by three so the sequence could not be read in triplets
424 (**Supplementary Table 1f**). The average Ka/Ks value per gene was used to assess the significance of the
425 sample median (**Supplementary Table 1g**).
426
427 **Data analysis**
428 Pan-genome analysis focused on a representative subset of 99 well-characterized accessions among the
429 original 339, including wild and American domesticated forms. In some cases, we also analysed the subset
430 of 114 European domesticated accessions (**Supplementary Table 5b**).
431 For GO enrichment, the annotated core genes and PAVs in the pan-genome were analysed using the
432 *buildGOmap* R function to infer indirect annotations and generate data suitable for *clusterProfiler* [61, 62].
433 Diagnostic genes were analysed using Metascape [63]. *A. thaliana* orthologs were identified using
434 OrthoFinder [58] and by comparing all protein sequences from *P. vulgaris* (v2.1) and *A. thaliana* (TAIR10).
435 For PCA, the PAV matrix (1/0) was analysed using the *logisticPCA* package in R [64].
436 ANOVA within subgroup M1 was carried out using the first principal component related to days-to-
437 flowering and photoperiod sensitivity [13] as a representative phenotypic trait.
438 F_{ST} analysis involved the separate testing of PAVs in the Mesoamerican and Andean gene pools by
439 comparing the frequency of each PAV between wild and domesticated forms. Each PAV was considered as
440 a single locus (0/1) and F_{ST} was calculated by applying the formula F_{ST} = (H total – H within) / H total, where
441 H is the heterozygosity [65]. The same procedure was applied to wild accessions when comparing the
442 Mesoamerican and Andean gene pools. Only PAVs in the top 5% of the F_{ST} distribution were considered as
443 candidates.
444 The functions of interesting PAVs and those associated with *A. thaliana* orthologs detected by OrthoFinder
445 [58] were investigated manually in the NCBI database (https://www.ncbi.nlm.nih.gov/).
446 Phylogenetic analysis involved the extraction and filtering of SNVs located in core genes and PAVs using
447 bcftools [59], resulting in two final datasets: 1,451,663 SNPs for the core genes and 338,475 SNPs for the
448 PAVs. The datasets were used to calculate the genetic distance between individuals and compute maximum
449 composite likelihood values with 1000 bootstraps for the NJ tree in MEGA11 [66]. The final trees were
450 visualized in FigTree (http://tree.bio.ed.ac.uk/software/figtree/).

451 The filtered dataset of SNPs in core genes was also used to quantify the genetic diversity within groups of
452 accessions by estimating π. The *--window-pi* vcftools flag was used to obtain measures of nucleotide
453 diversity in 250-kb windows. The windowed-*pi* estimates were then divided by the total number of SNPs to
454 calculate a global estimate for each genetic group.
455 Fisher's exact test with the false discovery rate corrected for multiple comparisons was applied in R to
456 identify PAVs that differed significantly in frequency between the Mesoamerican and Andean gene pools
457 for the American and European accessions.
458 The phenotypic data used for PAV-based GWAS encompassed the flowering time and photoperiod
459 sensitivity data previously analysed by Bellucci et al. [13]. GWA analysis was run by using both the Mixed
460 Linear Model (MLM) [67] and the Fixed and random model Circulating Probability Unification (FarmCPU)
461 [68] implemented in the R package GAPIT v3 [69]. The threshold for each Genome Wide Association (GWA)
462 scan was determined by the Bonferroni corrected *p* value at $\alpha = 0.05$. The kinship matrix (IBS method) was
463 calculated with Tassel 5 [70] and the population structure (at K2 obtained from Bellucci et al. [13]) were
464 included into the models as fixed factors. Quantile-quantile (Q-Q) plots were obtained by plotting the
465 observed -log10(*p* values) against the expected -log10(*p* values) under the null hypothesis of no association.
466

467 **Data Availability**

468 The 109 raw sequencing reads generated and analyzed in this study have been deposited in the Sequence
469 Read Archive (SRA) of the National Center of Biotechnology Information (NCBI) under BioProject number
470 PRJNA1042929. Additional data comprising 230 raw sequencing reads have been sourced from Frascarelli
471 et al. [11] and Bellucci et al. [13]. The pan-genome assembly and its annotation are publicly accessible via
472 this link: https://doi.org/10.6084/m9.figshare.24573874.
473

474 **References**

475 1. Broughton, W.J., Hernandez, G., and Blair, M.W. (2003) Beans (*Phaseolus* spp.) - Model food
476 legumes. *Plant and Soil*, 252(1):55-128. DOI: https://doi.org/10.1023/A:1024146710611

477 2. Myers, J.R. and Kmiecik, K. (2017). Common bean: economic importance and relevance to
478 biological science research. In: Pérez de la Vega, M., Santalla, M., and Marsolais, F. (eds) *The*
479 *Common Bean Genome*. Compendium of Plant Genomes. Springer, Cham. DOI:
480 https://doi.org/10.1007/978-3-319-63526-2_1

481 3. Bitocchi, E., Rau, D., Bellucci, E., Rodriguez, M., Murgia, M.L., Gioia, T., Santo, D., Nanni, L., Attene,
482 G., Papa, R. (2017) Beans (*Phaseolus ssp*.) as a model for understanding crop evolution. *Frontiers in*
483 *Plant Science,* 8:722. DOI: https://doi.org/10.3389/fpls.2017.00722

4. Intergovernmental Panel on Climate Change (IPCC) (2019). Climate Change and Land. Retrieved from https://www.ipcc.ch/srccl/

5. Gerten, D., Heck, V., Jägermeyr, J., Bodirsky, B.L., Fetzer, I., Jalava, M., Kummu, M., Lucht, W., Rockström, J., Schaphoff, S. et al. (2020) Feeding ten billion people is possible within four terrestrial planetary boundaries. *Nature Sustainability*, 3(3):200-208. DOI: https://doi.org/10.1038/s41893-019-0465-1

6. Bellucci, E., Mario Aguilar, O., Alseekh, S., Bett, K., Brezeanu, C., Cook, D., De la Rosa, L., Delledonne, M., Dostatny, D.F., Ferreira, J.J., et al. (2021) The INCREASE project: Intelligent Collections of food-legume genetic resources for European agrofood systems. *Plant Jour*nal, 108:646-660. DOI: https://doi.org/10.1111/tpj.15472

7. Cortinovis, G., Oppermann, M., Neumann, K., Graner, A., Gioia, T., Marsella, M., Alseekh, S., Fernie, A. R., Papa, R., Bellucci, E. et al.(2021). Towards the development, maintenance, and standardized phenotypic characterization of single-seed-descent genetic resources for common bean. *Current Protocols*, 1, e133. DOI: https://doi.org/10.1002/cpz1.133

8. Schmutz, J., McClean, P.E., Mamidi, S., Wu, G.A., Cannon, S.B., Grimwood, J., Jenkins, J., Shu, S., Song, Q., Chavarro, C., et al. (2014) A reference genome for common bean and genome-wide analysis of dual domestications. Nature Genetics, 46:707-713. DOI: https://doi.org/10.1038/ng.3008

9. Bitocchi, E., Nanni, L., Bellucci, E., Rossi, M., Giardini, A., Spagnoletti Zeuli, P., Logozzo, G., Stougaard, J., McClean, P., Attene, G., et al. (2012) Mesoamerican origin of the common bean (*Phaseolus vulgaris L.*) is revealed by sequence data. *Proceedings of the National Academy of Sciences,* 109(14):E788-E796. DOI: https://doi.org/10.1073/pnas.1108973109

10. Bitocchi, E., Bellucci, E., Giardini, A., Rau, D., Rodriguez, M., Biagetti, E., Santilocchi, R., Spagnoletti Zeuli, P., Gioia, T., Logozzo, G., et al. (2013) Molecular analysis of the parallel domestication of the common bean (*Phaseolus vulgaris*) in Mesoamerica and the Andes. *New Phytologist*, 197:300-313. DOI: https://doi.org/10.1111/j.1469-8137.2012.04377.x

11. Frascarelli, G., Galise, T.R., D'Agostino, N., Cafasso, D., Cozzolino, S., Cortinovis, G., Sparvoli, F., Bellucci, E., Di Vittori, V., Nanni, L., et al. (2023). The evolutionary history of the common bean (*Phaseolus vulgaris*) revealed by chloroplast and nuclear genomes. Preprint at *bioRxiv*, DOI: https://doi.org/10.1101/2023.06.09.544374

514 12. Cortinovis, G.; Frascarelli, G.; Di Vittori, V.; and Papa, R. (2020) Current state and perspectives in
515 population genomics of the common bean. Plants, 9, 330. DOI:
516 https://doi.org/10.3390/plants9030330

517 13. Bellucci, E., Benazzo, A., Xu, C., Bitocchi, E., Rodriguez, M., Alseekh, S., Di Vittori, V., Gioia, T.,
518 Neumann, K., Cortinovis, G., et al. (2023) Selection and adaptive introgression guided the complex
519 evolutionary history of the European common bean. *Nature Communications*, 14, 1908. DOI:
520 https://doi.org/10.1038/s41467-023-37332-z

521 14. Golicz, A.A., Batley, J., and Edwards, D. (2016) Towards plant pangenomics. *Plant Biotechnology*
522 *Journal*, 14:1099-1105. DOI: https://doi.org/10.1111/pbi.12499

523 15. Tranchant-Dubreuil, C., Rouard, M., and Sabot, F. (2019) Plant pangenome: impacts on phenotypes
524 and evolution. *Annual Plant Reviews*, DOI: 10.1002/9781119312994.apr0664

525 16. Furaste Danilevicz, M., Tay Fernandez, C.G., Marsh, J.I., Bayer, P.E., and Edwards, D. (2020) Plant
526 pangenomics: approaches, applications and advancements. *Current Opinion in Plant Biology*, 54:18-
527 25. DOI: https://doi.org/10.1016/j.pbi.2019.12.005

528 17. Khan, A.W., Garg, V., Roorkiwal, M., Golicz, A.A., Edwards, D., and Varshney, R.K. (2019) Super-
529 Pangenome by integrating the wild side of a species for accelerated crop improvement. *Trends in*
530 *Plant Science,* 25(2):148-158. DOI: https://doi.org/10.1016/j.tplants.2019.10.01p

531 18. Bellucci, E., Bitocchi, E., Ferrarini, A., Benazzo, A., Biagetti, E., Klie, S., Minio, A., Rau, D., Rodriguez,
532 M., Panziera, A., et al. (2014) Decreased nucleotide and expression diversity and modified
533 coexpression patterns characterize domestication in the common bean. *The Plant Cell*, 26(5):1901-
534 1912. DOI: https://doi.org/10.1105/tpc.114.124040

535 19. Luo, M., Tai, R., Yu, C.W., Yang, S., Chen, C.Y., Lin, W.D., Schmidt, W., and Wu K. (2015) Regulation
536 of flowering time by the histone deacetylase HDA5 in *Arabidopsis. The Plant Journal,* 82,925-936.
537 DOI: https://doi.org/10.1111/tpj.12868

538 20. Blanco, F.A., Peltzer Meschini, E., Zanetti, M.E., and Aguilar, O.M. (2009) A small GTPase of the Rab
539 family is required for root hair formation and preinfection stages of the Common bean–rhizobium
540 symbiotic association. *The Plant Cell*, 21(9):2797-2810. DOI:
541 https://doi.org/10.1105/tpc.108.063420

542 21. Dalla Via, V., Traubenik, S., Rivero, C., et al. (2017) The monomeric GTPase RabA2 is required for
543 progression and maintenance of membrane integrity of infection threads during root nodule
544 symbiosis. *Plant Molecular Biology*, 93:549-562. DOI: https://doi.org/10.1007/s11103-016-0581-5

545 22. Oladzad, A., González, A., Macchiavelli, R., de Jensen, C.E., Beaver, J., Porch, T., and McClean, P.
546 (2020) Genetic factors associated with nodulation and nitrogen derived from atmosphere in a
547 middle American common bean panel. *Frontiers in Plant Science*, 11:576078. DOI:
548 https://doi.org/10.3389/fpls.2020.576078

549 23. Ke, D., Fang, Q., Chen, C., Zhu, H., Chen, T., Chang, X., Yuan, S., Kang, H., Ma, L., Hong, Z., et al.
550 (2012) The small GTPase ROP6 interacts with NFR5 and is involved in nodule formation in Lotus
551 japonicus. *Plant Physiology*, 159(1):131-143. DOI: https://doi.org/10.1104/pp.112.197269

552 24. Corpas, F.J., Gupta, D.K., and Palma, J.M. (2021). Tryptophan: a precursor of signaling molecules in
553 higher plants. In: *Gupta, D.K., Corpas, F.J.* (eds) Hormones and Plant Response. Plant in Challenging
554 Environments, vol 2. Springer, Cham. DOI: https://doi.org/10.1007/978-3-030-77477-6_11

555 25. Morris, J.J., Lenski, R.E., and Zinser, E.R. (2012) The Black Queen Hypothesis: evolution of
556 dependencies through adaptive gene loss. *mBio*, 3(2):e00036-12. DOI:
557 https://doi.org/10.1128/mbio.00036-12

558 26. Wolf, Y.I. and Koonin, E.V. (2013) Genome reduction as the dominant mode of evolution. *Bioessays*,
559 35:829-837. DOI: https://doi.org/10.1002/bies.201300037

560 27. Suda, J., Meyerson, L.A., Leitch, I.J., and Pyšek, P. (2014). The hidden side of plant invasions: the
561 role of genome size. *New Phytologist,* 205:994-1007. DOI: https://doi.org/10.1111/nph.13107

562 28. Lavergne, S., Muenke, N.J., and Molofsky, J. (2010) Genome size reduction can trigger rapid
563 phenotypic evolution in invasive plants. *Annals of Botany,* 105(1):109-16. DOI:
564 https://doi.org/10.1093/aob/mcp271

565 29. Díez, C.M., Gaut, B.S., Meca, E., Scheinvar, E., Montes-Hernandez, S., Eguiarte, L.E., and Tenaillon,
566 M.I. (2013) Genome size variation in wild and cultivated maize along altitudinal gradients. *New*
567 *Phytologist,* 199:264-276. DOI: https://doi.org/10.1111/nph.12247

568 30. Hottes, A.K., Freddolino, P.R., Khare, A., Donnell, Z.N., Liu, J.C., and Tavazoie, S. (2013) Bacterial
569 adaptation through loss of function. *PLoS Genetics*, 9(7):e1003617. DOI:
570 https://doi.org/10.1371/journal.pgen.1003617

571 31. Albalat, R. and Cañestro, C. (2016) Evolution by gene loss. *Nature Reviews Genetics*, 17:379-391.
572 DOI: https://doi.org/10.1038/nrg.2016.39

573 32. Murray, A.W. (2020) Can gene-inactivating mutations lead to evolutionary novelty? *Current*
574 *Biology*, 30(10):R465-R471. DOI: https://doi.org/10.1016/j.cub.2020.03.072

575 33. Monroe, J.G., McKay, J.K., Weigel, D., and Flood, P.J. (2021) The population genomics of adaptive
576 loss of function. *Heredity*, 126:383-395, DOI: https://doi.org/10.1038/s41437-021-00403-2

577 34. Shimizu, K.K., Shimizu,-Inatsugi, R., Tsuchimatsu, T. and Purugganan, M.D. (2008), Independent
578 origins of self-compatibility in *Arabidopsis thaliana*. *Molecular Ecology*, 17:704-714. DOI:
579 https://doi.org/10.1111/j.1365-294X.2007.03605.x

580 35. Olson, M.V. (1999) When less is more: gene loss as an engine of evolutionary change. *American*
581 *Journal of Human Genetics,* 64:18-23. DOI: https://doi.org/10.1086/302219

582 36. Lutz, K.A., Wang, W., Zdepski, A, and Todd, P.M. (2011) Isolation and analysis of high-quality
583 nuclear DNA with reduced organellar DNA for plant genome sequencing and resequencing. *BMC*
584 *Biotechnology*, 11,54. DOI: https://doi.org/10.1186/1472-6750-11-54

585 37. Koren, S., Walenz, B.P., Berlin, K., Miller, J.R., Bergman, N.H., and Phillippy, A.M. (2017) Canu:
586 scalable and accurate long-read assembly via adaptive k-mer weighting and repeat separation.
587 *Genome Research*, 27(5):722–736, DOI: http://www.genome.org/cgi/doi/10.1101/gr.215087.116

588 38. Ruan, J. and Li, H. (2019) Fast and accurate long-read assembly with wtdbg2. *Nature Methods*,
589 17:155-158. DOI: https://doi.org/10.1038/s41592-019-0669-3

590 39. Vaser, R., Sović, I., Nagarajan, N., and Šikić, M. (2017) Fast and accurate de novo genome assembly
591 from long uncorrected reads. *Genome Research*, 27(5):737-746. DOI: 10.1101/gr.214270.116

592 40. Walker, B.J., Abeel, T., Shea, T., Priest, M., Abouelliel, A., Sakthikumar, S., Cuomo, C.A., Zeng, Q.,
593 Wortman, J., Young, S.K., et al. (2014) Pilon: an integrated tool for comprehensive microbial variant
594 detection and genome assembly improvement. *PloS One*, 9(11):e112963. DOI:
595 https://doi.org/10.1371/journal.pone.0112963

596 41. Simão, F.A., Waterhouse, R.M., Ioannidis, P., Kriventseva, E.V., and Zdobnov, E.M. (2015) BUSCO:
597 assessing genome assembly and annotation completeness with single-copy orthologs.
598 *Bioinformatics*, 31:3210-3212. DOI: https://doi.org/10.1093/bioinformatics/btv351

599 42. Cheng, H., Concepcion, G.T., Feng, X. Zhang, H., and Li, H. (2021). Haplotype-resolved *de novo*
600 assembly using phased assembly graphs with hifiasm. *Nature Methods,* 18,170–175. DOI:
601 https://doi.org/10.1038/s41592-020-01056-5

602 43. Li, H. (2018) Minimap2: pairwise alignment for nucleotide sequences. *Bioinformatics*, 34(18):3094-
603 3100. DOI: https://doi.org/10.1093/bioinformatics/bty191

604 44. Jayakodi, M., Padmarasu, S., Haberer, G., Bonthala, V.S., Gundlach, H., Monat, C., Lux, T.M., Kamal,
605 N., Lang, D., Himmelbach, A., et al. (2020) The barley pan-genome reveals the hidden legacy of
606 mutation breeding. *Nature*, 588:284-289. DOI: https://doi.org/10.1038/s41586-020-2947-8

607 45. Nattestad, M. and Schatz, M.C. (2016) Assemblytics: a web analytics tool for the detection of
608 variants from an assembly. *Bioinformatics,* 32:3021-3023. DOI:
609 https://doi.org/10.1093/bioinformatics/btw369

610 46. Li, H., Handsaker, B., Wysoker, A., Fennell, T., Ruan, J., Homer, N., Marth, G., Abecasis, G., Durbin R;
611 and 1000 Genome Project Data Processing Subgroup. (2009) The Sequence Alignment/Map format
612 and SAMTools. *Bioinformatics*, 25(16):2078-2079. DOI:
613 https://doi.org/10.1093/bioinformatics/btp352

614 47. Li, W. and Godzik, A. (2006) Cd-hit: a fast program for clustering and comparing large sets of
615 protein or nucleotide sequences. *Bioinformatics*. 22:1658-1659. DOI:
616 https://doi.org/10.1093/bioinformatics/btl158

617 48. Chen, S., Zhou, Y., Chen, Y., and Gu, J. (2018) fastp: an ultra-fast all-in-one FASTQ preprocessor.
618 *Bioinformatics*, 34(17): i884–i890. DOI: https://doi.org/10.1093/bioinformatics/bty560

619 49. Langmead, B. and Salzberg, S. (2012) Fast gapped-read alignment with Bowtie 2. *Nature Methods*,
620 9:357-359. DOI: https://doi.org/10.1038/nmeth.1923

621 50. Zimin, A.V., Marçais, G., Puiu,D., Roberts, M., Salzberg, S.L., and Yorke, J.A. (2013) The MaSuRCA
622 genome assembler. *Bioinformatics*, 29(21):2669-2677. DOI:
623 https://doi.org/10.1093/bioinformatics/btt476

624 51. Flynn, J., Hubley, R., Goubert, C., Rosen, J., Clark, A., Feschotte, C., and Smit, A.F. (2020)
625 RepeatModeler2 for automated genomic discovery of transposable element families. *Proceedings*
626 *of the National Academy of Sciences,* 117(17):9451-7. DOI:
627 https://doi.org/10.1073/pnas.1921046117

628 52. Tarailo-Graovac, M., and Chen, N. (2009) Using RepeatMasker to identify repetitive elements in
629 genomic sequences. *Current Protocols in Bioinformatics*, 4:4.10.1-4.10.14. DOI:
630 https://doi.org/10.1002/0471250953.bi0410s25

631 53. Hoff, K.J. and Stanke, M. (2019) Predicting Genes in Single Genomes with AUGUSTUS. *Current*
632 *Protocols in Bioinformatics*, ;65(1):e57. DOI: https://doi.org/10.1002/cpbi.57

633 54. Kim, D., Paggi, J., Park, C., Bennett, C., and Salzberg, S. (2019) Graph-based genome alignment and
634 genotyping with HISAT2 and HISAT-genotype. *Nature Biotechnology*, 37(8):907-15. DOI:
635 https://doi.org/10.1038/s41587-019-0201-4

636 55. Gremme, G., Brendel, V.P., Sparks, M.E., and Kurtz, S. (2005) Engineering a software tool for gene
637 structure prediction in higher organisms. *Information and Software Technology*, 47(15):965-978.
638 DOI: https://doi.org/10.1016/j.infsof.2005.09.005

639 56. Jones, P., Binns, D., Chang, H., Fraser, M., Li, W., McAnulla, C., McWilliam, H., Maslen, J., Mitchell,
640 A., Nuka, G., et al. (2014) InterProScan 5: genome-scale protein function classification.
641 *Bioinformatics,* 30(9):1236-40. DOI: https://doi.org/10.1093/bioinformatics/btu031

642 57. Altschul, S., Gish, W., Miller, W., Myers, E., and Lipman, D. (1990) Basic local alignment search tool.
643 *Journal of Molecular Biology,* 215:403-10. DOI: https://doi.org/10.1016/S0022-2836(05)80360-2

644 58. Emms, D.M., and Kelly, S. (2019) OrthoFinder: phylogenetic orthology inference for comparative
645 genomics. *Genome Biology*, 20(1):238. DOI: https://doi.org/10.1186/s13059-019-1832-y

646 59. Li, H. (2011) A statistical framework for SNP calling, mutation discovery, association mapping and
647 population genetical parameter estimation from sequencing data. *Bioinformatics*, 27(21):2987-
648 2993. DOI: https://doi.org/10.1093/bioinformatics/btr509

649 60. Wang, D., Zhang, Y., Zhang, Z., Zhu, J. and Yu, J. (2010) KaKs_Calculator 2.0: a toolkit incorporating
650 gamma-series methods and sliding window strategies. *Genomics Proteomics & Bioinformatics*, 8:77-
651 80. DOI: https://doi.org/10.1016/S1672-0229(10)60008-3

652 61. Yu, G., Wang, L., Han, Y., and He, Q. (2012) clusterProfiler: an R package for comparing biological
653 themes among gene clusters *OMICS: A Journal of Integrative Biology*, 16(5):284-287. DOI:
654 https://doi.org/10.1089/omi.2011.0118

655 62. Wu, T., Hu, E., Xu, S., Chen, M., Guo, P., Dai, Z., Feng, T., Zhou, L., Tang, W., Zhan, L., et al. (2021).
656 clusterProfiler 4.0: A universal enrichment tool for interpreting omics data. *The Innovation*,
657 2(3):100141. DOI: https://doi.org/10.1016/j.xinn.2021.100141

658 63. Zhou, Y., Zhou, B., Pache, L., Chang, M., Khodabakhshi, A.H., Tanasichuk, O., Benner, C., Chanda,
659 S.K. (2019) Metascape provides a biologist-oriented resource for the analysis of systems-level
660 datasets. *Nature Communication*, 10,1523. DOI: https://doi.org/10.1038/s41467-019-09234-6

661 64. Landgraf, A.J. and Lee, Y. (2020) Dimensionality reduction for binary data through the projection of
662 natural parameters. *Journal of Multivariate Analysis,* 180:104668. DOI:
663 https://doi.org/10.1016/j.jmva.2020.104668

65. Wright, S. (1951) The genetical structure of populations. *Annals of Eugenics*, 15:323-354. DOI: https://doi.org/10.1111/j.1469-1809.1949.tb02451.x

66. Tamura, K., Stecher, G., and Kumar, S. (2021) MEGA11: Molecular evolutionary genetics analysis. *Molecular Biology and Evolution*, 38(7):3022-3027. DOI: https://doi.org/10.1093/molbev/msab120

67. Yu, J., Pressoir, G., Briggs, W.H., Vroh Bi, I., Yamasaki, M., Doebley, J.F., McMullen, M.D., Gaut, B.S., Nielsen, D.M., Holland, J.B., et al. (2006). A unified mixed-model method for association mapping that accounts for multiple levels of relatedness. *Nature Genetics,* 38(2):203-8. DOI: https://doi.org/10.1038/ng1702

68. Liu, X., Huang, M., Fan, B., Buckler, E.S., and Zhang, Z. (2016). Iterative usage of fixed and random effect models for powerful and efficient genome-wide association studies. *PLoS Genetics,* 12(2):e1005767. DOI: https://doi.org/10.1371/journal.pgen.1005767

69. Wang, J. and Zhang, Z. (2021). GAPIT Version 3: Boosting Power and Accuracy for Genomic Association and Prediction. *Genomics Proteomics Bioinformatics*, 19(4):629–40. DOI: https://doi.org/10.1016/j.gpb.2021.08.005

70. Bradbury, P.J., Zhang, Z., Kroon, D.E., Casstevens, T.M., Ramdoss, Y., and Buckler, E.S. (2007) TASSEL: software for association mapping of complex traits in diverse samples. *Bioinformatics,* 23(19):2633-5. DOI: https://doi.org/10.1093/bioinformatics/btm308

682 **Figures**

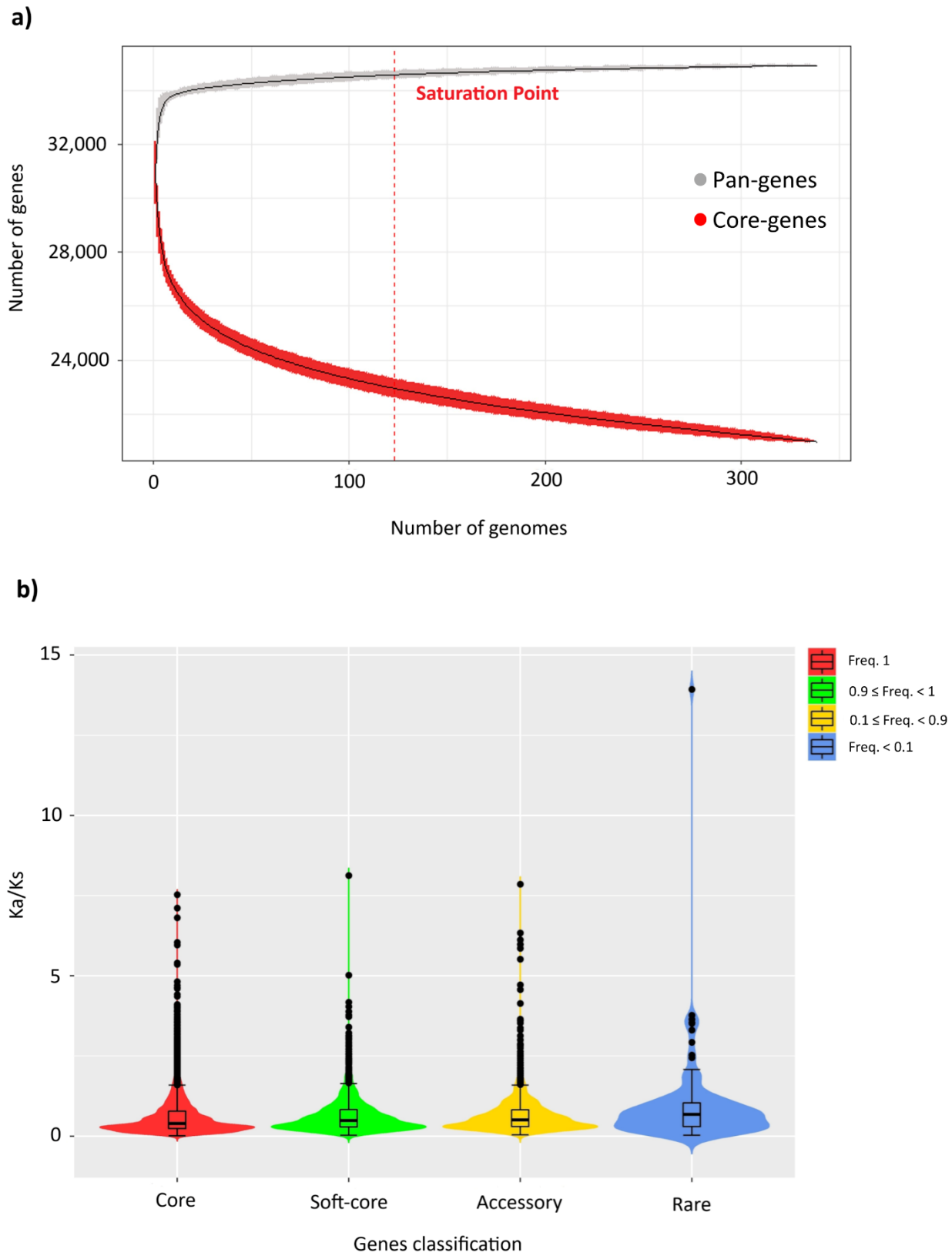

683

684 **Fig. 1: Characterization of the common bean pan-genome. a,** Pan-gene and core gene size calculation. The

685 growth curve of pan-genes (grey) reached saturation point (99%, 34,579 genes) when 120 individuals were

686 included, as indicated by the dashed red line. In contrast, the growth curve of core genes (red) diminished
687 with the addition of each genotype. **b,** Violin plots showing analysis of variance (ANOVA) related to the
688 ratio of non-synonymous to synonymous mutations in the core genes and PAs. The PAVs are split into three
689 subcategories based on their frequency: soft core, accessory, and rare. **Supplementary Table 1g** contains
690 detailed statistics.

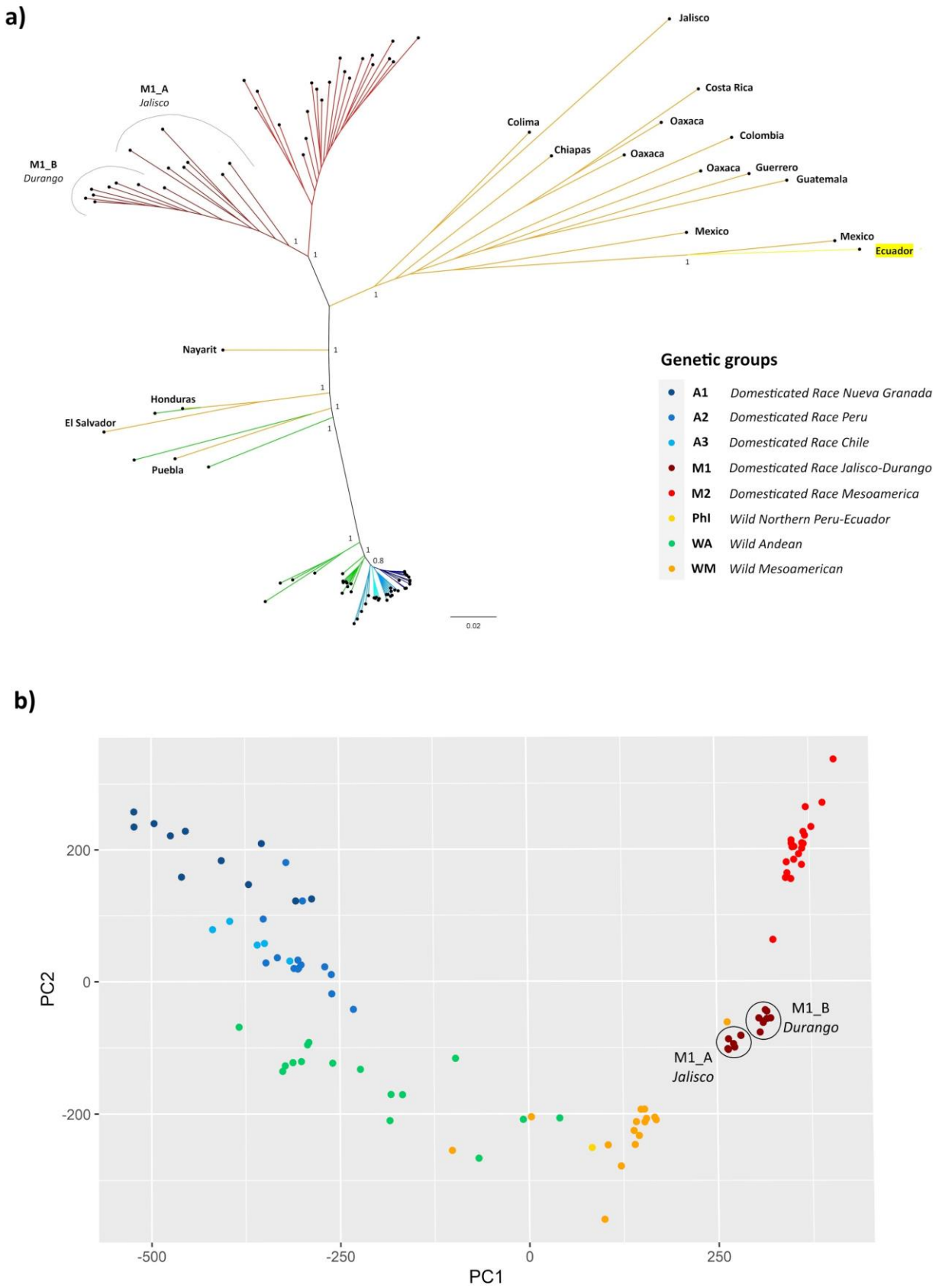
a)
M1_A
Jalisco
M1_B
Durango
Jalisco
Costa Rica
Colima
Oaxaca
Colombia
Chiapas
Oaxaca
Oaxaca
Guerrero
Guatemala
Mexico
Mexico
Ecuador
Nayarit
Honduras
El Salvador
Puebla
0.02
Genetic groups
A1 Domesticated Race Nueva Granada
A2 Domesticated Race Peru
A3 Domesticated Race Chile
M1 Domesticated Race Jalisco-Durango
M2 Domesticated Race Mesoamerica
PhI Wild Northern Peru-Ecuador
WA Wild Andean
WM Wild Mesoamerican
b)
PC2
PC1
200
0
-200
-500
-250
0
250
M1_B
Durango
M1_A
Jalisco

691

c)

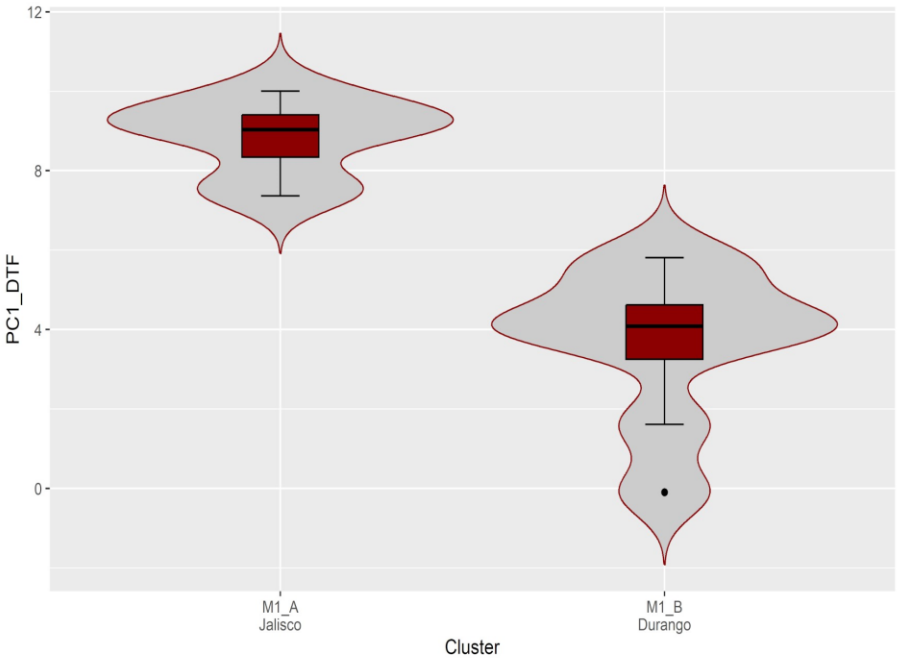
12
8
4
0
PC1_DTF
M1_A
Jalisco
M1_B
Durango
Cluster

d)

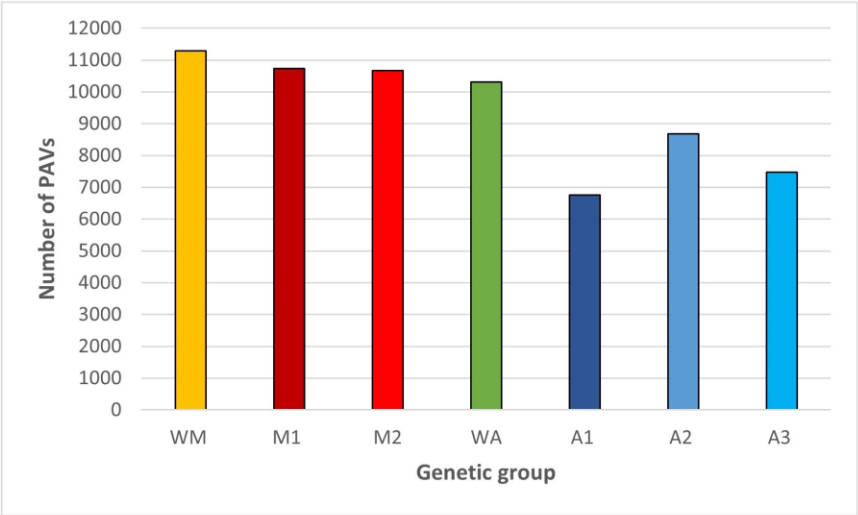
12000
11000
10000
9000
8000
7000
6000
5000
4000
3000
2000
1000
0
Number of PAVs
WM
M1
M2
WA
A1
A2
A3
Genetic group

e)

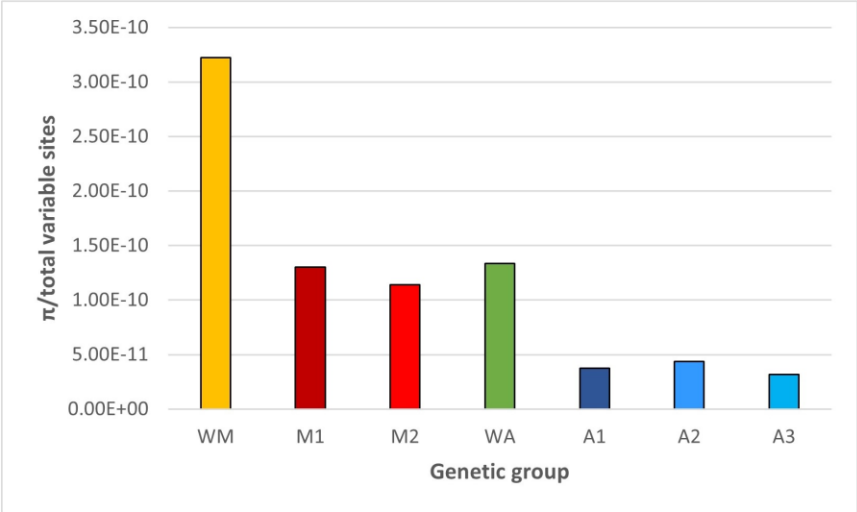
3.50E-10
3.00E-10
2.50E-10
2.00E-10
1.50E-10
1.00E-10
5.00E-11
0.00E+00
π/total variable sites
WM
M1
M2
WA
A1
A2
A3
Genetic group

692

693 **Fig. 2: Population structure of *P. vulgaris*. a,** Neighbour-joining (NJ) phylogenetic tree constructed using
694 only SNPs located in core genes (bootstrap = 1000). **b,** PAV-based principal component analysis (PCA). **c,**
695 Violin plots showing the analysis of variance (ANOVA) for PC1 representing days to flowering and
696 photoperiod sensitivity in the M1/Jalisco-Durango races by splitting the accessions into two clusters based
697 on PCA and the NJ tree. **d,** Bar chart showing the number of PAVs per genetic group. **e,** Bar chart showing
698 nucleotide diversity calculated by estimating π in 250-kb windows. All procedures were applied to a
699 representative subset of 99 genetically and phenotypically well-characterized *P. vulgaris* accessions.

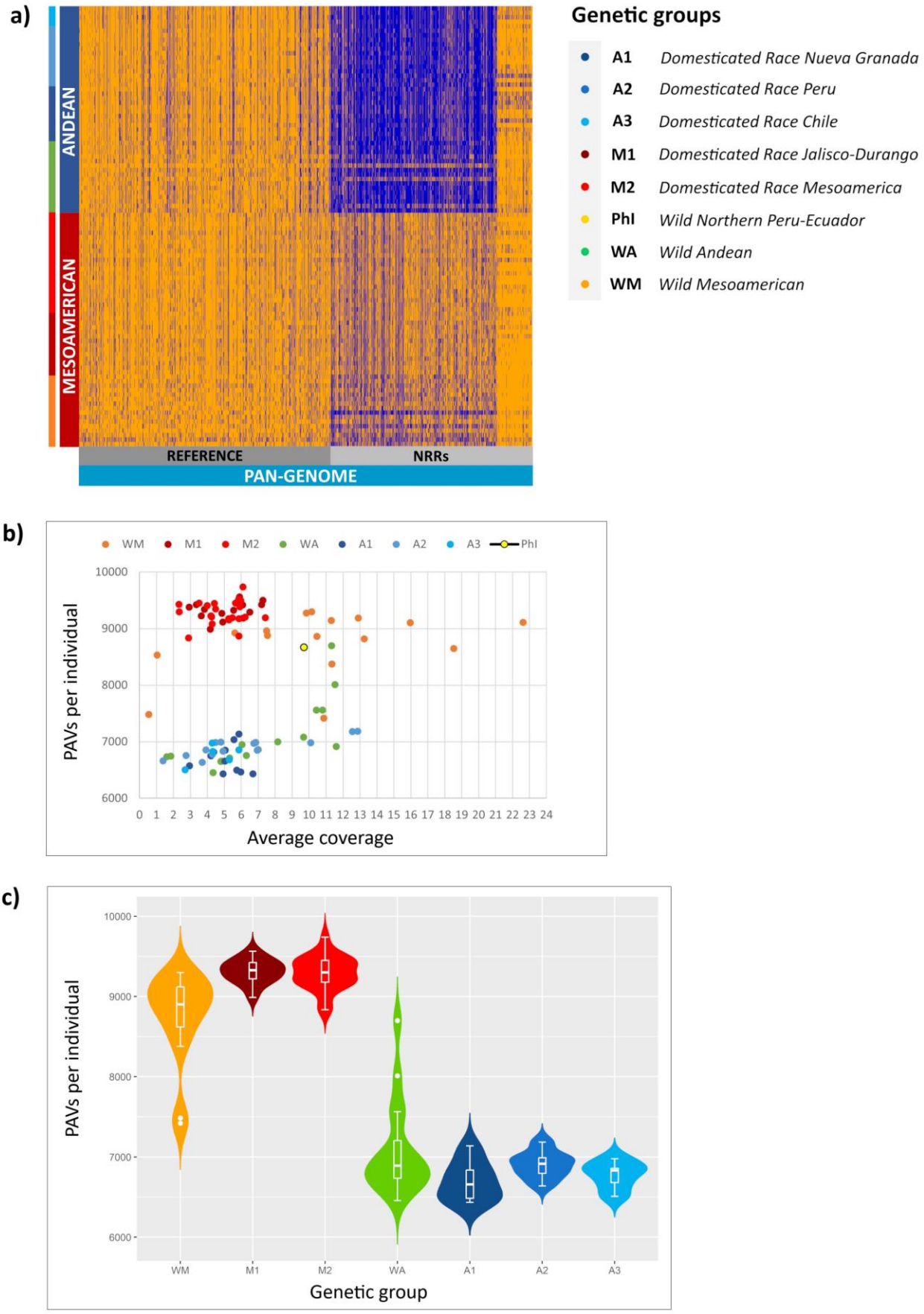
a)
ANDEAN
MESOAMERICAN
REFERENCE
NRRs
PAN-GENOME
Genetic groups
A1 Domesticated Race Nueva Granada
A2 Domesticated Race Peru
A3 Domesticated Race Chile
M1 Domesticated Race Jalisco-Durango
M2 Domesticated Race Mesoamerica
PhI Wild Northern Peru-Ecuador
WA Wild Andean
WM Wild Mesoamerican
b)
WM M1 M2 WA A1 A2 A3 PhI
PAVs per individual
Average coverage
c)
PAVs per individual
Genetic group
WM M1 M2 WA A1 A2 A3

700

701 **Fig. 3: Evolution of the common bean pan-genome. a,** Heat map illustrating the number of PAVs per
702 individual in the final pan-genome. Orange indicates presence while blue indicates absence. **b,** Scatterplot
703 showing the number of PAVs per individual (y-axis) in relation to the coverage (x-axis) of each genotype. **c,**
704 Violin plots representing the analysis of variance (ANOVA) for the number of PAVs per individual by genetic
705 group. All procedures were applied to a representative subset of 99 genetically and phenotypically well-
706 characterized *P. vulgaris* accessions. **Supplementary Table 3a** contains detailed statistics.

707

a)

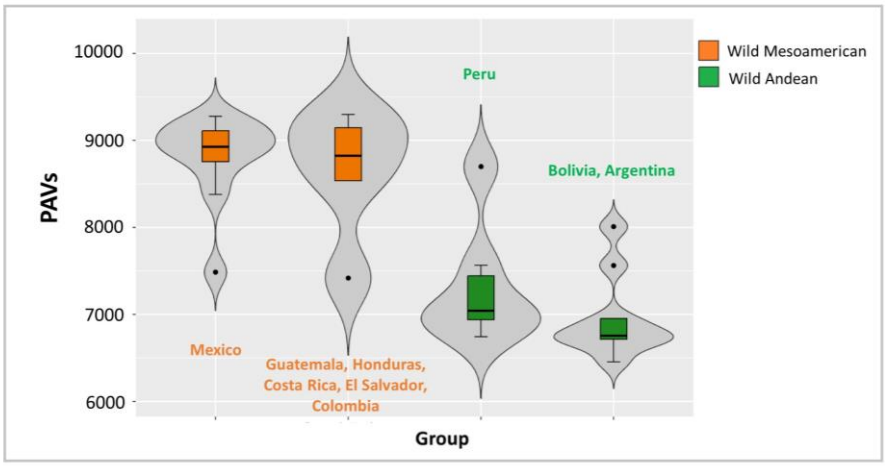
Wild Mesoamerican
Wild Andean
PAVs
10000
9000
8000
7000
6000
Peru
Bolivia, Argentina
Mexico
Guatemala, Honduras, Costa Rica, El Salvador, Colombia
Group

b)

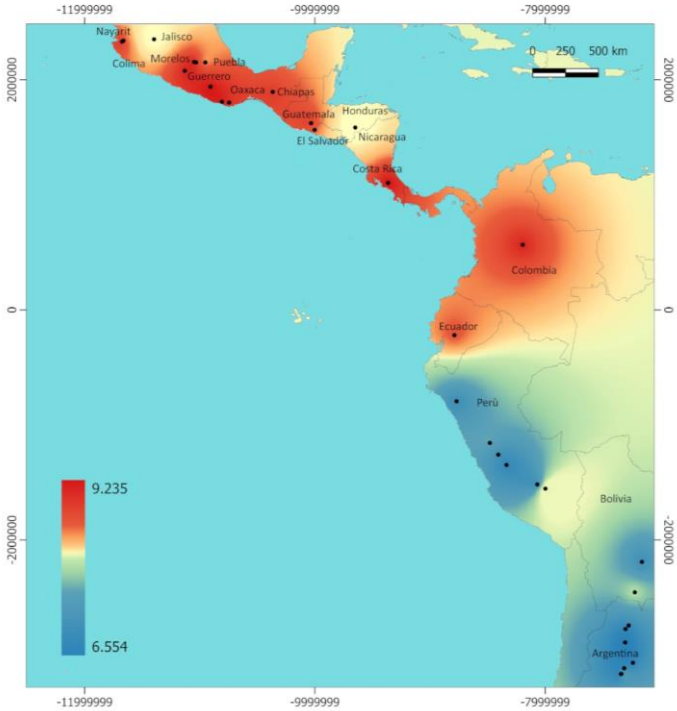
-11999999
-9999999
-7999999
2000000
0
-2000000
Nayarit
Jalisco
Colima
Morelos
Puebla
Guerrero
Oaxaca
Chiapas
Guatemala
Honduras
El Salvador
Nicaragua
Costa Rica
0 250 500 km
Colombia
Ecuador
Perù
Bolivia
Argentina
9.235
6.554

c)

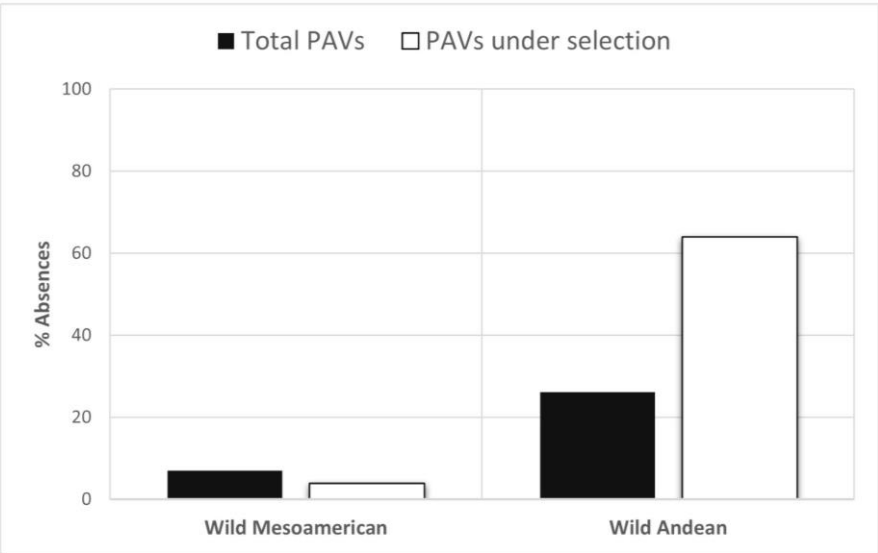
Total PAVs
PAVs under selection
% Absences
100
80
60
40
20
0
Wild Mesoamerican
Wild Andean

708

709 **Fig. 4: Selection for adaptive gene loss during the expansion of wild common bean. a,** Violin plots showing
710 the analysis of variance (ANOVA) for the number of PAVs per individual based on grouping the wild
711 Mesoamerican and Andean accessions according to latitude coordinates. **Supplementary Table 3b** contains
712 detailed statistics. **b,** Interpolation of the geographic distributions of the wild accessions based on the
713 number of PAVs per individual. Dark red regions indicate a higher number of PAVs and blue regions a lower
714 number of PAVs. **c,** Bar charts showing the proportions of absences found for the subset of PAVs putatively
715 under selection during the wild expansion (white) and for the entire variable genome (black).

716

a)

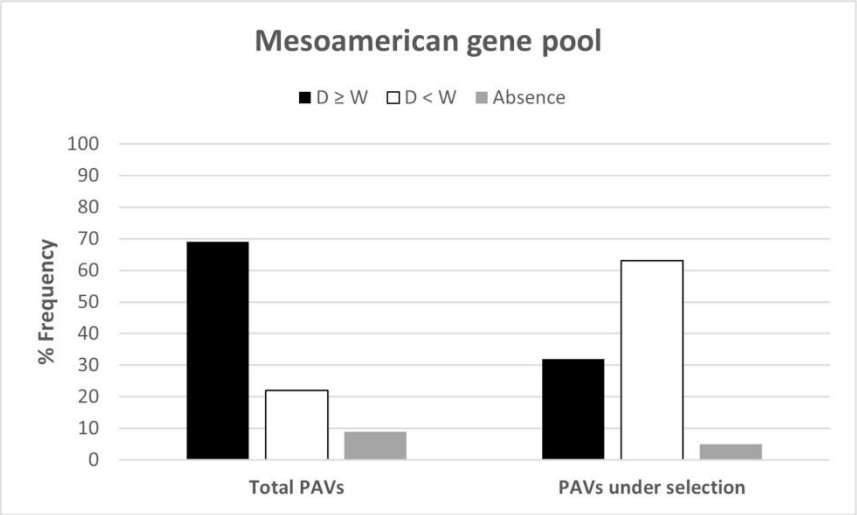

b)

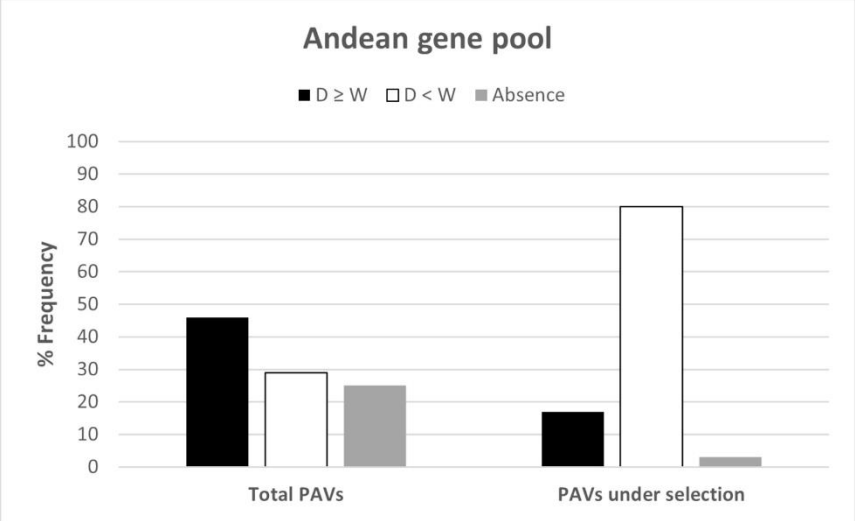

717

718 **Fig. 5: Localized adaptive reduction effects during the domestication of the common bean. a,** Bar chart
719 showing the proportions of presence/absence in the Mesoamerican gene pool for the entire variable

720 genome (left) and for the subset of PAVs putatively under selection between wild and domesticated
721 populations (right). **b,** Bar chart showing the proportions of presence/absence in the Andean gene pool for
722 the entire variable genome (left) and for the subset of PAVs putatively under selection between wild and
723 domesticated populations (right). In both charts, the presence values are divided based on frequency (≥/<)
724 in the comparison between wild and domesticated forms.